

# Shaping Optical Microresonators on the Surface of Optical Fibers With Negative Effective Radius Variations

Dmitry V. Krisanov, Alexander S. Nesterok , and Ilya D. Vatnik

**Abstract**—We examine moderate CO<sub>2</sub> laser heating as a method of forming negative effective radius variations in conventional optical fiber. Fiber samples were subjected to focused CO<sub>2</sub> laser radiation in the form of 100 ms pulses with power 0.36 to 1.3 W and thermalization time up to 2.2 s. Fiber temperatures reached 200 to 300 degrees Celsius in each pulse. The temperatures are significantly smaller than the glass transformation temperature, which is nearly 1500 °C. We show that short CO<sub>2</sub> laser pulses may introduce negative variations up to 5 nm. The magnitude of the introduced variation increases roughly linearly for up to 6 pulses, and then fiber saturation is achieved. We reveal that it is possible to produce optical whispering gallery modes resonators in low-temperature heating mode and create a triangular-shape microresonator solely with the negative variations. The negative variations may also occur in peripheral areas of high-temperature heated fiber while introducing positive effective radius variations. To eliminate it, we propose low-temperature fiber annealing before high-temperature variations introducing. The negative variations may also be implemented to develop a new independent approach of shaping optical whispering gallery modes microresonators.

**Index Terms**—Nanophotonics, optical fibers, optical resonators, whispering gallery modes.

## I. INTRODUCTION

IT IS known that the cladding of the standard telecommunication fiber can support long-living whispering gallery modes [1], [2]. Microresonators of such modes (also referred to as «resonators of surface nanoscale optical photonics» or «SNAP» [3]) appear to be a promising platform for new types of photonic microdevices [4], [5]. The attraction of the microresonators is in the possibility to control the speed of axial propagation of the whispering gallery modes (WGM) with tiny changes in the effective radius of the optical fiber: variations distributed along the axis of the system play the role of one-dimensional potential wells for wave packets of WGM [6].

Up to date, several methods have been demonstrated for precise modification of the optical fiber shape. Permanent nanoscale

positive variations of the fiber's effective radius can be introduced with CO<sub>2</sub> laser heating [7], UV exposure of photosensitive fibers [8], femtosecond laser modification [9], fiber bending [10]. Using a CO<sub>2</sub> or a femtosecond laser to introduce the permanent variations is considered a conventional technique [11]. Both techniques present the increment of the effective radius only. At the same time, some SNAP devices such as a microresonators chain [12] may be easily manufactured if negative variations are introduced rather than positive ones. It was noted that the negative change in the effective radius might follow the positive one under the influence of sufficiently high-power laser radiation [13]. However, the practical application of such an approach is questionable. Recently, etching in the hydrofluoric acid of the partially uncoated fiber has been proposed as a method to introduce substantial negative variations [14]. However, the method based on etching a masked optical fiber sample implies only rectangular modifications.

Here we reveal that the typical way of creating SNAP devices with annealing by a CO<sub>2</sub> laser may also cause the introduction of the negative variations in the radius instead of positive ones. We have found that the negative variations may appear at temperatures well below the glass transformation temperature. We show that the proposed regime is suitable for producing the surface axial nanoscale photonic devices, potentially having some advantages due to the lower temperature impact on the sample material.

## II. EXPERIMENTAL METHODS AND SETUP

We utilize a setup that is similar to those described in [13]. The system comprises a 36 W Synrad CO<sub>2</sub> laser with an output beam diameter of 3.5 mm, and an optical shutter with less than 10 ms opening time. A system of mirrors followed by a plano-convex cylindrical Zn-Se lens that focuses the laser radiation on the surface of a fiber. The fiber sample is moved along its axis using a linear positioner with a minimum step of 2.5 μm (see Fig. 1). Given the focal length of 2.5 cm, the estimated waist diameter of the laser beam after the lens was 50 μm with the Rayleigh length of the order of 1 mm.

The utilizing of the optical shutter ensures that the heating occurs in a controllable manner and at a small-time scale. The shutter allows forming a short pulse of a well reproducible duration of 100 ms. Then one can determine the introduced value of the effective radius variation by the number of pulses

Manuscript received August 20, 2021; revised September 29, 2021; accepted October 14, 2021. Date of publication October 19, 2021; date of current version November 2, 2021. This work was supported in part by the Russian Foundation for Basic Research under Grant RFBR, 20-32-10170, and in part by Ministry of Education and Science of the Russian Federation under Grant FSUS-2020-0034. (Corresponding author: Alexander S. Nesterok.)

The authors are with the Fiber Laser Laboratory, Physics Department, Novosibirsk State University, Novosibirsk 630090, Russia (e-mail: chrisdi@email.su; al509@mail.ru; ilya.vatnik@gmail.com).

Digital Object Identifier 10.1109/JPHOT.2021.3121039

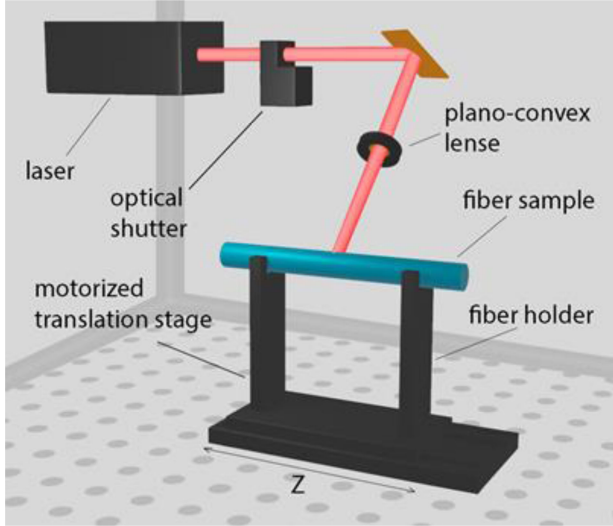


Fig. 1. Experimental setup of irradiation of the microresonator based on optical fiber with CO<sub>2</sub> laser.

applied to the point of the sample. The pulse period was 1.5 s to ensure that the sample thermalizes between the pulses. The use of short optical pulses instead of continuous-wave radiation provides a well-reproducible temperature profile in the impact region. Moreover, it makes the modification area more confined, as thermal diffusion plays a lesser role.

As the samples, we used the standard Corning SMF-28 telecommunication optical fiber with a cladding diameter of 125  $\mu\text{m}$ . To prepare the microresonator sample, we removed the secondary plastic cladding using a thermal stripper. Then the cleaned surface was treated with ethylene glycol.

We estimate the temperatures reached during the modification process using a one-dimensional heat transfer equation [15]:

$$\frac{dT}{dt} = \frac{k}{c_p \rho^2} T'' - \frac{(T - T_0) 2h}{c_p \rho^2} - \frac{2\sigma (T^4 - T_0^4)}{c_p \rho^2} + \frac{\sqrt{2}P}{\pi^{3/2} \omega_x c_p \rho r^2} e^{-\frac{2x^2}{\omega_x^2}} \text{erf} \left( \sqrt{2} \frac{r_f}{\omega_y} \right), \quad (1)$$

where:

- $k$  quartz glass thermal conductivity;
- $c_p$  heat capacity;
- $\rho$  density;
- $T$ , sample temperature;
- $T_0$  environment temperature;
- $h$  heat transfer constant;
- $\sigma$  Stefan-Boltzmann constant;
- $\omega_x, \omega_y$  transverse dimensions of the laser spot in the focal plane;
- $r$  sample radius;
- $P$  total power of the laser radiation.

The first term on the right-hand side of this equation is responsible for heat transfer along the fiber. The second term characterizes the convective heat exchange of the sample with the environment, the third term considers the radiation losses, and the fourth term is the heat source from the laser beam.

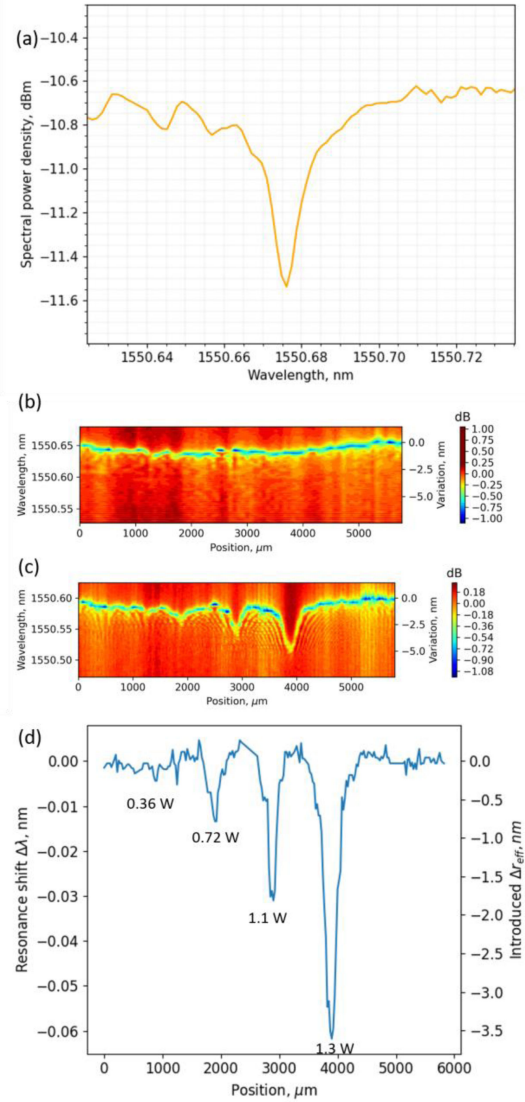


Fig. 2. (a) A typical pristine sample transmission spectrum. (b) Transmission spectra at the different points along the pristine sample. (c) The same for the sample after irradiation with single laser pulses of 0.1 s duration with different powers. (d) The introduced negative variations of the effective radius.

To measure the introduced variations of the effective radius, we use a conventional technique of measuring the spectra of the whispering gallery modes at the different points along the fiber [16]. For this, a thin tapered optical fiber (taper) with a waist diameter of few microns is used to excite the WGM in the optical fiber sample. The transmission spectrum through the taper comprises a plenty of resonances, each corresponding to the different axial, azimuthal, and radial modes, with a typical Q-factor of  $10^{5-6}$  (Fig. 2(a)). As the free spectral range for axial numbers is much smaller than for azimuthal numbers, it's possible to designate a single azimuthal series of axial numbers in the spectrum. Within this series, the spectral position  $\lambda(z)$  of the mode with the smallest axial number varies with the effective radius variations as

$$\Delta\lambda(z) = \lambda \frac{\Delta r_{eff}(z)}{r} n, \quad (2)$$

where  $n$  is the refractive index.

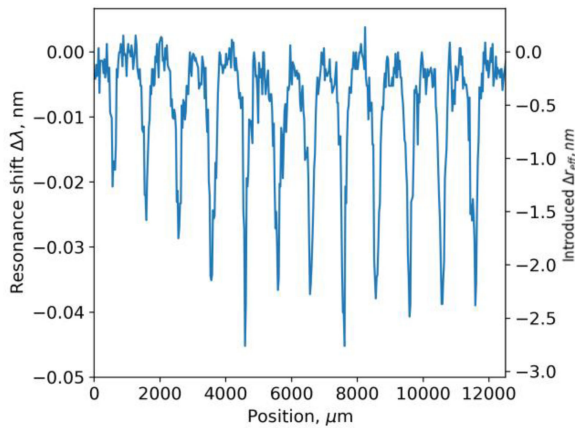


Fig. 3. The effective radius variation introduced at the different points of the sample with the different number of pulses. From left to right – from 1 to 12 pulses. The laser power is 0.72 W.

### III. RESULTS AND DISCUSSION

We have found that for the specific parameters of the modification process, the effective radius does decrease instead of increasing. To demonstrate this, we subject the sample of the microresonator to a single 100 ms pulse of focused  $\text{CO}_2$  radiation with four different powers – 0.36, 0.72, 1.11, 3 W at the different points of the sample distant from each other for 1 mm. We have measured the spectra of WGM before and after modification and found that heating has decreased the fiber effective radius. According to Fig. 2(b), the maximum resonant wavelength differs in different points even for unmodified fiber, forming initial radius variation up to 1 nm.

Whereas irradiation with a power of 0.4 W did not lead to distinguishable changes in the effective radius, higher powers led to a dip in the effective radius axial profile.

We estimated the temperatures achieved with such a short radiation impact as 200–300 °C, which is significantly lower than the transformation temperature of silica glass. We suppose that the effect may correspond to a decrease of the refractive index. Indeed, it was noticed that with moderate heating below transformation temperature with subsequent rapid cooling, the refractive index of glasses could slightly reduce [17]. So, this mechanism differs from previously described inducing the positive effective radius variation [13] with the release of the frozen tensions.

We then have checked the scalability of the introduced variation with several impulses applied to the same point of the sample. We set the power to 0.72 W; the optical shutter was opened for 0.1 seconds with time between consequent pulses of 2.2 seconds. We applied from 1 to 12 pulses in different points at 1 mm from each other and then calculate introduced modifications depth as the difference between the axial profiles of the pristine effective radius variation  $\Delta r_{\text{eff}}(z)$  the and the modified samples.

We found that the value of the introduced variation increases roughly linearly for up to 5 pulses, after which it reaches the value of approximately 2.5 nm and does not increase any more, demonstrating the saturation (see Fig. 3).

Despite the overall saturation, there are slight deviations of the introduced  $\Delta r_{\text{eff}}(z)$  for the many-pulse modifications (right

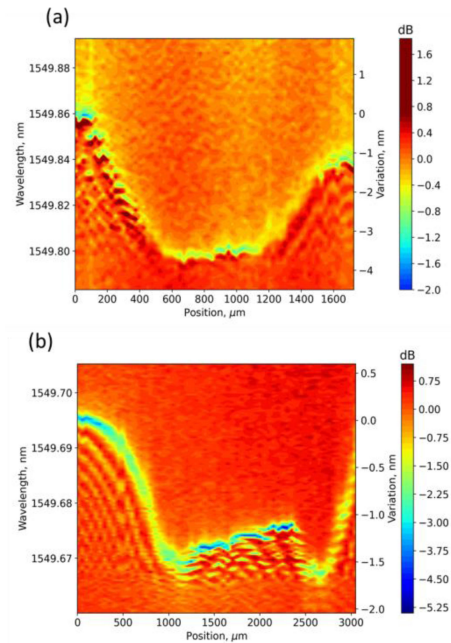


Fig. 4. (a) Transmission spectra for a WGM microresonator with uniform shape obtained due to saturation. (b) Transmission spectra for a microresonator with linearly increasing effective radius made solely with negative variations.

part of Fig. 3). That occurs as the laser power fluctuates by 1% with a typical time of a minute. That, in turn, means that different modifications are created at the slightly different laser powers and possess different saturation levels.

The saturation of the introduced variations can be utilized to obtain modifications with the uniform shape. Indeed, to reproduce this type of axial profile, it is sufficient to apply a large enough number of pulses to the required section of the fiber sample. To demonstrate this, we apply 20 pulses each 60  $\mu\text{m}$  of the sample at the laser power of 1 W and obtain a SNAP resonator with part of almost uniform shape (see Fig. 4(a)).

The linear part of the dependence, presented in Fig. 3, may be utilized for controllable modification of the SNAP device. To demonstrate these capabilities, we made a sample that has a part with the linearly growing effective radius solely with negative variations. To demonstrate this, we recorded a modification of a triangular-shaped fiber sample. It consists of 19 points located along the axis of the microresonator every 100  $\mu\text{m}$ ., we exposed the first and the last five modification points to 15 laser impulses to separate the place of the recorded modification from the rest of the sample. The triangular modification itself consists of nine points, at which the optical shutter opened from 10 times at the lowest point to 1 time at the top. We entirely produced the modification at a laser power of 1.3 W, the shutter opening time was 100 ms, and the thermalization time after each opening was 2200 ms. The resulted modification does have a part with linearly increasing variation, showing the fundamental suitability of reducing the effective radius to create SNAP microresonators with arbitrary shapes.

It should also be noted that the negative variations of the effective radius also occur in the high-temperature regime, which is used to introduce the positive variations. When the

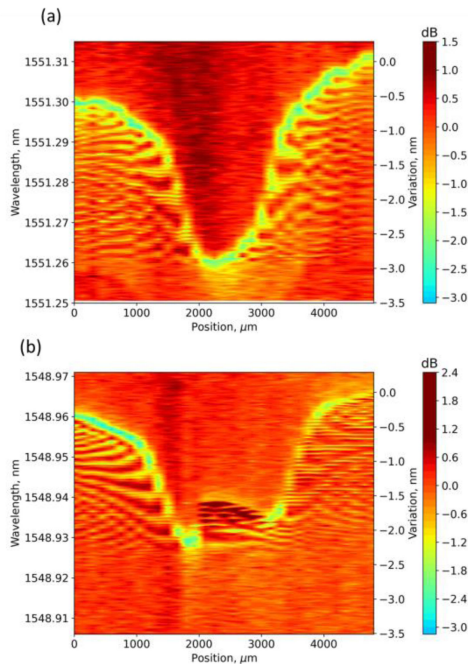


Fig. 5. (a) Transmission spectra for the microresonator treated with continuous-wave laser beam slightly below the threshold power for the positive variations (with temperatures below transformation temperature). (b) The spectra for the sample treated with laser with the higher power leading to the temperatures above the transformation temperature.

sample is heated to high temperatures, some peripherally heated regions always have temperatures lower than the transformation one. Depending on the pulse duration, laser beam parameters, the fiber radius, this peripheral area may be smaller or larger than the central spot subjected to the positive variations. To demonstrate the presence of both areas with both negative and positive variations, we made a modification with the continuous irradiation with the laser power slightly lower and higher than the threshold of positive variations of 3 W that we defined above. The stages slowly moved the sample under the laser beam, which irradiates an area of 1 mm. For high enough irradiation intensity, we observed that the positive variation follows the negative (compare Fig. 5(a) and Fig. 5(b)). Note that the part of the microresonator with high-temperature treatment that experienced positive variations demonstrates the Fano-type resonances when exciting the whispering gallery modes [18]. That may occur due to changing the surface properties with high-intensity irradiation with ablation [15].

The coexistence of both the negative and the positive variations requires preparing a fiber sample to introduce the positive variations without side effects. To do this, one should preliminarily anneal it with moderate-intensity irradiation to saturate all the possible negative variations in the whole sample. This method also increases the surface quality [15].

#### IV. CONCLUSION

We demonstrated here that  $\text{CO}_2$  laser irradiance may decrease the effective radius of the optical fiber cladding supporting the whispering gallery modes. The effect appears if the

sample is heated to temperatures well below the transformation temperature, estimated with a numerical model to be around  $300^\circ\text{C}$ . We have shown that there is a maximum achievable value of the negative variation of the radius given a particular heating/cooling regime. The minimum and the maximum values of the introduced variation achieved in the experiments were 0.6-5 nm, respectively.

We have shown the method's feasibility by creating the SNAP microresonator that possesses a region with the linearly growing effective radius variation. Thus, the effect of the negative variations should be considered when introducing the variations using other heating techniques and can also be utilized as the independent method to shape the SNAP devices.

#### ACKNOWLEDGMENT

The authors thank D. V. Kudashkin for the fruitful discussion and characterization of the samples.

#### REFERENCES

- [1] A. W. Poon, R. K. Chang, and J. A. Lock, "Spiral morphology-dependent resonances in an optical fiber: Effects of fiber tilt and focused Gaussian beam illumination," *Opt. Lett.*, vol. 23, no. 14, Jul. 1998, Art. no. 1105.
- [2] V. A. Sychugov, V. P. Torchigin, and M. Y. Tsvetkov, "Whispering-gallery waves in optical fibres," *Quantum Electron.*, vol. 32, no. 8, pp. 738–742, Aug. 2002.
- [3] M. Sumetsky and J. M. Fini, "Surface nanoscale axial photonics," *Opt. Exp.*, vol. 19, no. 27, Dec. 2011, Art. no. 26470.
- [4] M. Sumetsky and M. J. Li, "Nanophotonics of optical fibers," *Nanophotonics*, vol. 2, no. 5–6, pp. 393–406, Jan. 2013.
- [5] V. V. Dvoyrin and M. Sumetsky, "Bottle microresonator broadband and low-repetition-rate frequency comb generator," *Opt. Lett.*, vol. 41, no. 23, Dec. 2016, Art. no. 5547.
- [6] M. Sumetsky, "Theory of SNAP devices: Basic equations and comparison with the experiment," *Opt. Exp.*, vol. 20, no. 20, Sep. 2012, Art. no. 22537.
- [7] M. Sumetsky *et al.*, "Surface nanoscale axial photonics: Robust fabrication of high-quality-factor microresonators," *Opt. Lett.*, vol. 36, no. 24, Dec. 2011, Art. no. 4824.
- [8] M. Sumetsky, D. J. DiGiovanni, Y. Dulashko, X. Liu, E. M. Monberg, and T. F. Taunay, "Photo-induced SNAP: Fabrication, trimming, and tuning of microresonator chains," *Opt. Exp.*, vol. 20, no. 10, 2012, Art. no. 10684.
- [9] Q. Yu, S. Zaki, Y. Yang, N. Toropov, X. Shu, and M. Sumetsky, "Rectangular SNAP microresonator fabricated with a femtosecond laser," *Opt. Lett.*, vol. 44, no. 22, Nov. 2019, Art. no. 5606.
- [10] D. Bocek, N. Toropov, I. Vatnik, D. V. Churkin, and M. Sumetsky, "SNAP microresonators introduced by strong bending of optical fibers," *Opt. Lett.*, vol. 44, no. 13, Jul. 2019, Art. no. 3218.
- [11] M. Sumetsky, "Optical bottle microresonators," *Prog. Quantum Electron.*, vol. 64, pp. 1–30, Mar. 2019.
- [12] M. Sumetsky, "A SNAP coupled microresonator delay line," *Opt. Exp.*, vol. 21, no. 13, Jul. 2013, Art. no. 15268.
- [13] M. Sumetsky and Y. Dulashko, "SNAP: Fabrication of long coupled microresonator chains with sub-angstrom precision," *Opt. Exp.*, vol. 20, no. 25, Dec. 2012, Art. no. 27896.
- [14] N. Toropov, S. Zaki, T. Vartanyan, and M. Sumetsky, "Microresonator devices lithographically introduced at the optical fiber surface," *Opt. Lett.*, vol. 46, no. 7, Apr. 2021, Art. no. 1784.
- [15] M. H. Lai, K. S. Lim, D. S. Gunawardena, Y. S. Lee, and H. Ahmad, " $\text{CO}_2$  laser applications in optical fiber components fabrication and treatment: A review," *IEEE Sensors J.*, vol. 17, no. 10, pp. 2961–2974, May 2017.
- [16] M. Sumetsky and Y. Dulashko, "Radius variation of optical fibers with angstrom accuracy," *Opt. Lett.*, vol. 35, no. 23, Dec. 2010, Art. no. 4006.
- [17] H. J. Hoffmann, W. W. Jochs, and N. M. Neuroth, "Relaxation phenomena of the refractive index caused by thermal treatment of optical glasses below  $T_g$ ," *Properties and Characteristics of Optical Glass*, vol. 0970, Jan. 1989, Art. no. 2.
- [18] S. B. Gorajooobi, G. S. Murugan, and M. N. Zervas, "A general model for taper coupling of multiple modes of whispering gallery resonators and application to analysis of coupling-induced fano interference in a single cavity," *Opt. Exp.*, vol. 27, no. 18, Sep. 2019, Art. no. 25493.